


Biosynthesis, characterization, and applications of aluminum oxide nanoparticles using aqueous extract of Cinnamon

Waleed K. Mahdi ; Aqeel O. Flayyih; Falih H. Musa

AIP Conf. Proc. 3219, 050006 (2024)

<https://doi.org/10.1063/5.0236391>



View
Online



Export
Citation

Articles You May Be Interested In

Honey/polymeric nanofiber enriched with clove (*Syzygium aromaticum* L.) extract and Al₂O₃ nanoparticles: Antibacterial and in vitro wound healing studies

AIP Conference Proceedings (August 2022)

Synthesis and characterization of metal nanoparticles from the bark of *Cinnamomum zeylanicum* (Ceylon cinnamon)

AIP Conf. Proc. (July 2019)

Preparation of silver oxide nanoparticles using cinnamon plant by green synthesis method and its biological applications

AIP Conf. Proc. (December 2023)

Biosynthesis, Characterization, and Applications of Aluminum oxide Nanoparticles using Aqueous Extract of Cinnamon

Waleed K. Mahdi^{1,a)}, Aqeel O. Flayyih^{2,b)}, and Falih H. Musa^{3,c)}

¹ Department of Chemistry, College of Education of Pure Science, Ibn – Al Haitham, University of Baghdad, Baghdad-Iraq.

²Lecturer in the Ministry of Education. Baghdad-Iraq.

³The head of Department of Medical Laboratory Techniques, Ashur University College. Baghdad-Iraq

^{a)} Correspondence author: waleed.k.m@ihcoedu.uobaghdad.edu.iq

^{b)} oqil.awda1205a@ihcoedu.uobaghdad.edu.iq,

^{c)} falih.hassan@au.edu.iq

Abstract: The α - Al₂O₃Nps has successfully been synthesized by the green method using aluminum nitrate. nona hydrate Al(NO₃)₃·9H₂O, cinnamon extract in sodium hydroxide. The green synthesis is less expensive, produces less pollution, and enhances environmental and human health safety, it is more advantageous than traditional chemical synthesis. These nanoparticles were identified by spectroscopy (Ft-IR), UV-vis spectroscopy, (X-Ray diffraction-(XRD)), (Scanning Electron Microscopy- (SEM)), (Transmission Electron Microscope- (TEM)), (Energy Dispersive X-ray-(EDX)), and (Atomic Force Microscopy-(AFM)). Based on the obtained results, synthesized α - Al₂O₃Nps was in a rhombohedral phase with an average diameter (62.71 nm). The efficiency of the α - Al₂O₃Nps to various antimicrobial activities was examined for resistance to the bacteria *Escherichia coli*, *Staphylococcus aureus*, and *Candida albicans*. using the diffusion method of agar. The inhibition zone values indicate that nanoparticles effect on different bacteria. The efficiency results of the synthesized α - Al₂O₃Nps as an adsorbent were tested by immersing α - Al₂O₃Nps into a solution of divalent ions of (Cobalt, Nickel, and Copper) the percentage of the removal of these ions were Co^(II) 91.25%, Ni^(II) 84.42%, Cu^(II) 93.81%. The percentage of the metal ions removal was measured by using UV-visible spectroscopy.

INTRODUCTION

Recent research has shown that Both industry and biomedicine frequently use nanoparticles. Aluminum oxide nanoparticles, also known as alumina nanoparticles, are an intriguing subset of the family of metal oxide nanoparticles. They can be made using a variety of techniques, including sol-gel, precipitation, micro-emulsion, and hydrothermal methods. [1]. In the latter half of the 20th century, aluminum oxide (alumina) was one of the most significant engineering materials due to its special properties, which included chemical stability, a high melting point, and high hardness [2]. it has been concluded that the Measurements of the mechanical, thermal, and density characteristics. cause Increased Cu-coated Al₂O₃ nanoparticles to have a significant impact on composite samples. The microstructure, hardness, compressive strength, and thermal expansion properties are all improved by the Al₂O₃ that has been coated with Cu and is distributed well in the Al matrix. But the addition of Cu-coated Al₂O₃ has a worsened impact on densification and ductility [3]. Moreover, α - Al₂O₃Nps also find extensive biomedical applications in biosensors [4], biofiltration [5], and drug delivery [6]. There are many easy ways to synthesize (Al₂O₃Nps) such as: laser ablation, hydro thermal, sol-gel, mechanical chemical [7-11] In addition to these methods, green chemistry can be used as an environmentally friendly, less energy-consuming and highly efficient method, in which plant components are used in parts. Plants such as roots, stems, flowers and fruits, where these parts play a dual role in biological synthesis, including its role as a stabilizer for Nb and as a natural reducing agent for the synthesis of Al₂O₃Nps in different sizes and

forms. In the year 2019, Suresh Ghotekar studied the plants used for the green synthesis of $\text{Al}_2\text{O}_3\text{Nps}$ with their applications and diagnosis using appropriate techniques. [12]. Ravichandran. S. et al prepared $\text{Al}_2\text{O}_3\text{Nps}$ by using a size of 200-400nm for biosynthesis using neem leaves (*Azadirachta indica*) as a plant extract that has wide applications in the field of immunotherapy, cancer treatment, and many diseases. It is also used in the field of biomedicine such as drug delivery. [13]. Hakuta. Y. et al successfully prepared the rod-like of (α - $\text{Al}_2\text{O}_3\text{Nps}$) by using boehmite nanoparticles and using supercritical water conditions for hydrothermal phase transformation g. [8]. Ismail .R et al, [14] synthesized $\text{Al}_2\text{O}_3\text{Nps}$ and showed the co-existence of the α - Al_2O_3 and γ - Al_2O_3 phases by laser ablation of an aluminum target in ethanol. Narayanan.V.M and, Rakesh .S . G [15], synthesized alumina Nps using aluminum nitrate and lemon extract with an average size of 460 nm. Manyasree. D. et al [16] using Sodium hydroxide and aluminum sulphate with a crystal size of 35 nm to prepare the alumina nanoparticles. The biological activity was also evaluated by antimicrobial testing using *Escherichia coli*, which showed at (50 mg/ml) concentration the highest inhibition zone, which is 39 mm from $\text{Al}_2\text{O}_3\text{Nps}$. At low concentrations (1 $\mu\text{g/ml}$), the α - $\text{Al}_2\text{O}_3\text{Nps}$ demonstrated significant toxicity toward a dominant microbial species (*Bacillus licheniformis*). [17,18]. Sathiya Narayanan N et, al [19] examine how the texture of the cemented carbide tool affects the main cutting force, thrust force, and coefficient of friction when cutting austenitic stainless steel 304. Both nanoparticles and non-nanoparticles are filled in the texture gaps. In comparison to a conventional and textured tool, the combined effect of surface texturing and lubrication with Al_2O_3 nanoparticles improved the performance of the cutting tool. Tok. A I .Y, et al [20] have revealed a low-cost flame spray pyrolysis technique to create agglomerated free nano -sized Al_2O_3 with a size of (5-30nm) .The aim of the work is used of facile green method to synthesis of α - $\text{Al}_2\text{O}_3\text{Nps}$ by using aluminum nitrate. nonahydrate , sodium hydroxide with plant extract (Cinnamon) , which is distinguished by various methods to support the product α - $\text{Al}_2\text{O}_3\text{Nps}$ and investigated their antibacterial activity of (*Staphylococcus aureus* , *Escherichia coli* and *Candida albicans* -fungal) to give a good efficiency of α - $\text{Al}_2\text{O}_3\text{Nps}$ as adsorbent for divalent metal ions (Cobalt , Nickel and Copper). So the targets of green manufacturing is limit the amount of pollutants they produce or release during operation. reduce emissions of greenhouse gases. Eliminate or drastically cut down on the production of waste. Gather, repurpose, recycle, or compost waste.

MATERIALS AND METHODS

Cinnamon was procured from a local market and source. ($\text{Al}(\text{NO}_3)_3 \cdot 9\text{H}_2\text{O}$) (Germany / Merck), NaOH from (India / Alpha chemical) , Absolute ethanol (RBL-Spain), (CoSO_4 Cobalt sulfate , $\text{CuSO}_4 \cdot 5\text{H}_2\text{O}$ Copper sulfate. pentahydrate $\text{CuSO}_4 \cdot 5\text{H}_2\text{O}$ and Nickel sulfate. Heptad hydrate $\text{NiSO}_4 \cdot 7\text{H}_2\text{O}$.) (Merck – Germany) and deionized distilled water. All chemicals are employed without additional purification. Cinnamon was taken from Baghdad locally market (they usually collected as shown in Fig. 1).

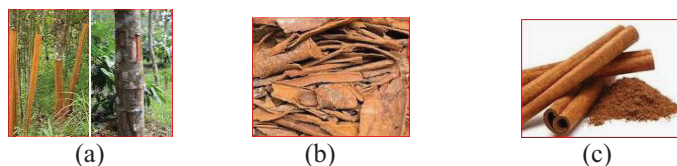


FIGURE 1. a) Cinnamon tree, b) Cinnamon plant bark, (c) Cinnamon powder.

Preparation of Plant Extract

Making fresh cinnamon extract is the first step. To get rid of any impurities, the cinnamon is rinsed by deionized water then dried at laboratory temperature. After thoroughly mixing, a 500 mL beaker containing 200 mL of deionized water and cinnamon was heated at 70 °C for 30 minutes and then the plant solution extracted was allowed to cool to room temperature, it turned from colorless to light brown. The filter paper type Whatman No: 1 was used to filter the mixture. In a 1.5 ml tube, the centrifuged was used to separate the resulting solution for (15 min) at (4000 rpm). A stock solution containing cinnamon extract was obtained.

Synthesis and Characterization of α -Al₂O₃Nps

Al(NO₃)₃.9H₂O weight (3.75g) was dissolved in 30 ml of deionized water, followed by the addition of 100 ml of cinnamon extract as a dispersant, stirring, and heating at a temperature of 70 C⁰. After that, a solution of sodium hydroxide (1M) was gradually added to the mixture drop by drop until the PH = 12. The resulting was allowed to precipitate for (48 hr), forming a brown precipitate that was spun apart using a centrifuge, washed with (deionized water, hot ethanol), and dried for (10hr) in an electric oven at 300 C⁰, resulting in a white powder of α -Al₂O₃ Nps. The method used to create α -Al₂O₃Nps powder using an aqueous extract of Cinnamon is illustrated in Fig. 2.



FIGURE 2. The preparation steps of α -Al₂O₃Nps powder using Cinnamon extract.

Various approaches were used to identify α -Al₂O₃Nps. as follows: Electronic Balance , (A 220 /C / 1 model), PLC Centrifuge (4000 – 4500 rpm), (FAITHFUL) Electric oven, water bath with shaking (SCL F), Tape of pH, the spectrum of (160/UV) Shimadzu spectrophotometer. The studies of FT-IR have been recorded by using (8500S) type Shimadzu in the range (400 – 4000cm⁻¹) from Baghdad University, and (XRD) (Holland/ Phillips) in the laboratories center of Baghdad. (SEM) Scanning Electron Microscope type (300 Hv / Germany-Z. S), (EDX), (TEM) type (100Kv / Germany), at (Kashan University / Iran). Atomic Force Microscopy (AFM), type (Nano surf AG . Liestal), Switzerland was carried out at the University of Baghdad / College of Science. Disc diffusion technique in a nutrient medium (jellose medium). The α -Al₂O₃Nps was tested for its antimicrobial properties against two reference *Staphylococcus* bacterial strains using Mueller Hinton agar., and (G-) *Escherichia coli* and (G+) *aureus* as well as *Candida albicans* fungal, and the same procedure for antifungal activity using potato dextrose as a nutrient medium (agar). Adsorption measurements were carried out by using (UV-vis) spectrophotometer type (160/UV) Shimadzu spectrophotometer.

Antibacterial Method

(Gram-negative(-ev) and gram-positive (+ev) bacteria), specifically (*Escherichia coli*, and *Staphylococcus aureus* as well as the fungus *Candida albicans*), are the pathogenic bacterial strains in this study. α -Al₂O₃ antibacterial activity was evaluated using the agar well diffusion method. LB agar (luria Bertani agar) was seeded with 24-hour incubated cultures of the respective clinical isolates and the individual bacterial strains were spread separately on the agar medium. Nutrient media was then poured into sterilized petri dishes. Each petri plate has a well of 6 mm diameter that is made using a sterile cork borer in an aseptic environment. *Candida albicans* fungal, was carried out by the technique of disc diffusion in a (jellose- medium) nutrient medium of the (MHA: Mueller Hinton agar) variety, as well as the same technique for antifungal activity PDA for potato dextrose. The biological activity of the nanoparticles is evaluated using various concentrations (i.e., 2mg/ml, 1mg/ml, 0.5mg/ml, and 0.25mg/ml). Using sterile micropipettes, the nanoparticles are mixed with sterile water before being added to wells. After that, plates were incubated for (36hr at 37 C⁰). Each well's zone of inhibition was measured after the incubation period, and the results were recorded. Values were calculated in millimeters (mm) for the ultimate antibacterial activity.

Adsorption Method

This study was carried out by using α - Al_2O_3 Nps as adsorbent with a selected divalent metal ions (Cobalt, Nickel and Copper) with about 5ppm of solution concentration, which were made by proper dilution of stock solution and was agitated for half an hour with pH =6. The effect of the divalent ions of (Cobalt , Nickel and Copper) was studied by different concentrations from 1 to 10 mg /L and 0.5 gm. of adsorbent, at contact time from 1- 30 min. There was an increase in the adsorption and then it was almost stable, after that there was a decrease in the percentage of bio absorption.

RESULTS AND DISCUSSIONS

An aqueous extract of Cinnamon was used with $\text{Al}(\text{NO}_3)_3 \cdot 9 \text{H}_2\text{O}$. The changing color solutions are shown in (See Fig. 3a) from pale brown to brown in (See Fig. 3b), and after that to dark brown in (See Fig. 3c), and also a white powder of α - Al_2O_3 Nps in (See Fig. 3d).

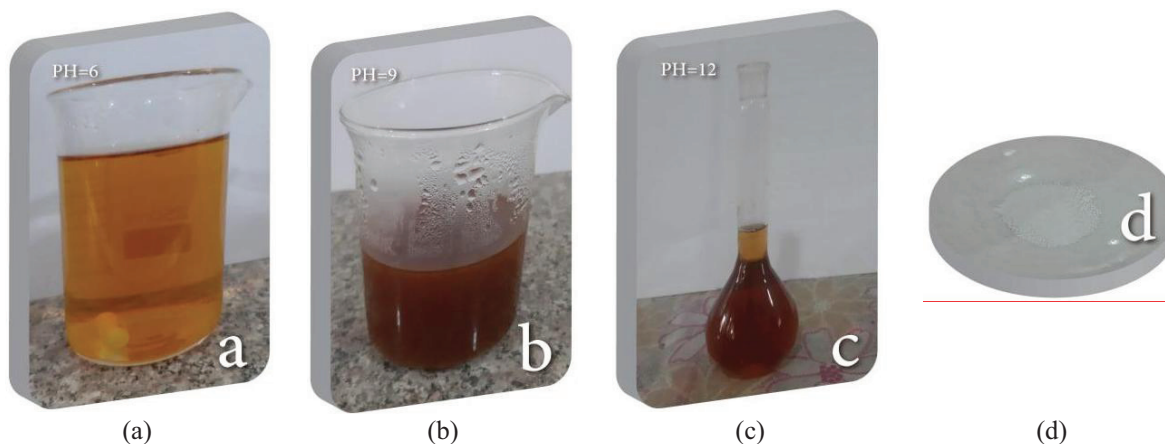


FIGURE 3. Color change of solutions of $\text{Al}(\text{NO}_3)_3 \cdot 9 \text{H}_2\text{O}$ and bio-reductor of Cinnamon extract, a) pale brown, b) brown, c) dark brown, and d) α - Al_2O_3 Nps powder.

From the FT-IR spectrum of α - Al_2O_3 Nps showed, O-H bands and C-H bond vibration are responsible for the weak broadband at 3468 cm^{-1} and 2300 cm^{-1} . Bands at 574 cm^{-1} and 447 cm^{-1} , which referred to the Al-OH group's bending vibration (Al-O). Additionally, the 624 cm^{-1} peak represented the Al - O band's stretching vibration. [21][22]. Crystallization of alumina also showed a band at 732 cm^{-1} due to the stretching frequency of Al-O-Al for octahedral coordinated aluminum [23], as shown in Fig. 4.

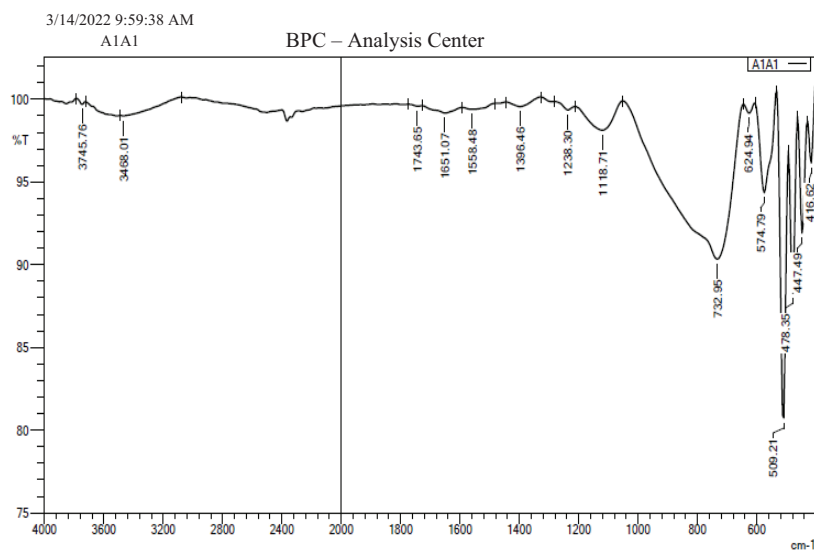


FIGURE 4. Ft - IR spectrum of α - Al_2O_3 Nps powder

The electronic spectrum showed an absorption peak for α - $\text{Al}_2\text{O}_3\text{Nps}$ at ($\lambda_{\text{max}}= 252 \text{ nm}$) of UV region. Estimates of the optical energy band gap (E_g) were made by $1239.83 / 252 = 4.91 \text{ eV}$ as shown in Fig. 5. [24].

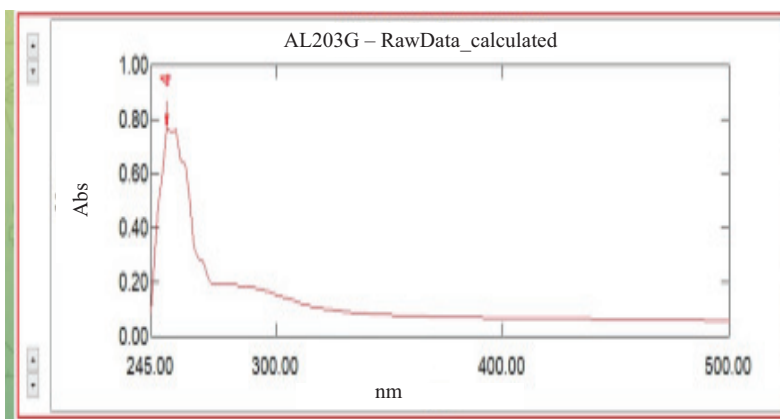


FIGURE 5. UV – vis absorption spectrum of α - $\text{Al}_2\text{O}_3\text{Nps}$ powder

XRD for the phase formation and crystallite size. As shown in the XRD pattern (Fig. 6), diffraction peaks can be indexed associated with 2θ : 27.74° , 32.44° , 46.78° , 54.08° and 68.41° (300) with index Miller of (012), (104), (202), (024) and (300) respectively.

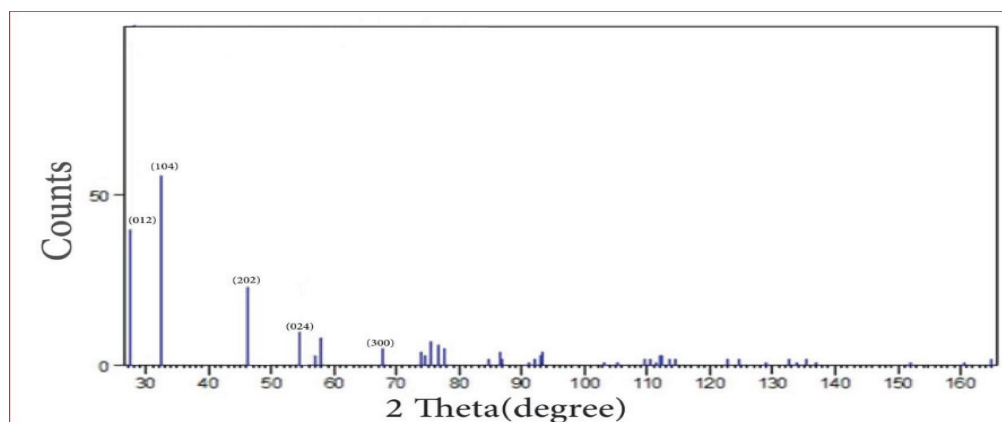


FIGURE 6. XRD of α - $\text{Al}_2\text{O}_3\text{Nps}$ powder.

The crystallite size is determined using Debye-Scherer's method $d = K \lambda / \beta \cos \theta$ [24][7], d : represented, the average crystalline dimension perpendicular to the reflective phases, (λ : wavelength of x-ray), and (K : Scherer's constant) (0.92), to calculate the full width at half maximum (FWHM) (β) of the diffraction peaks. When instrumental broadening is excluded, a Bragg reflection's, (FWHM: full width at half maximum) where (θ is the Bragg's angle). The products' calculated average crystallite size was discovered in the range (62.71 nm). The sample's rhombohedral structure is revealed by the obtained diffraction to be crystalline, matching reference pattern JCPDS files:10 – 0173 and 50- 0173 as shown in Table 1. [25].

TABLE 1. XRD analysis results of α - $\text{Al}_2\text{O}_3\text{Nps}$ powder.

2-Theta	hkl	FWHM	XS (nm)	Average of Crystallite Size (nm)
27.749	012	0.638	13.49	13.266 nm
32.443	104	0.492	17.57	
46.781	202	1.067	8.48	
54.081	024	0.618	15.08	
68.418	300	0.857	11.71	

Morphological study of SEM and TEM showed, Fig. 7 (a and b) that the size and the morphology of synthesized (α - Al_2O_3 Nps) was shaped like a plate, it was non-spherical shape and had a uniform size and distribution, with a particle size (51.95 – 73.27 nm). The average particle size is (62.71 nm). [26][27].

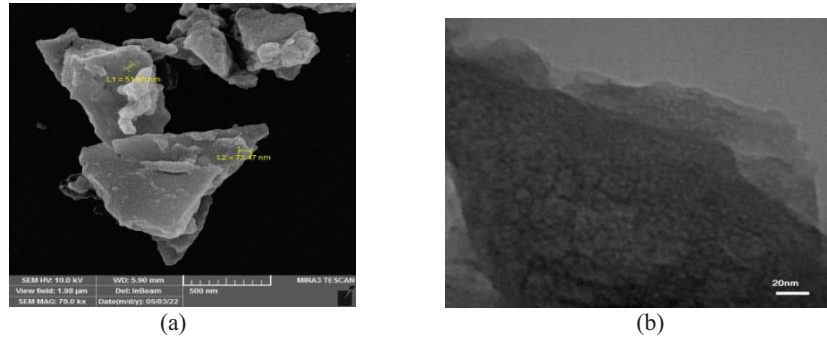


FIGURE 7. (a) SEM, and (b) TEM image of α - Al_2O_3 Nps powder

The EDX results for α - Al_2O_3 Nps. Fig 8. showed that Al and O's existence is abundantly clear. There were no observable impurities in the alumina, which indicated it was chemically pure [28].

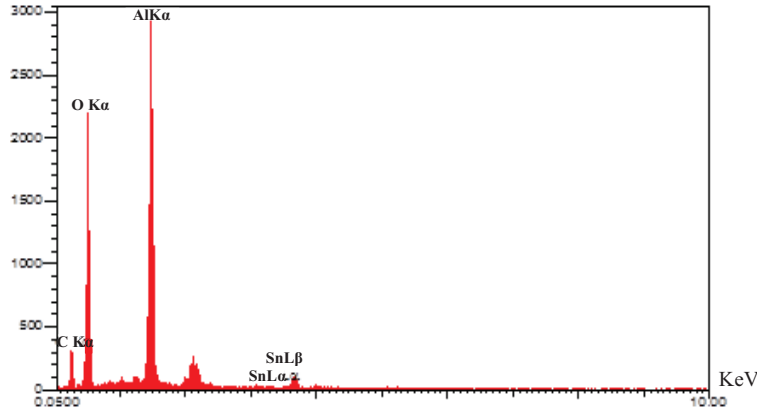


FIGURE 8. EDX results for α - Al_2O_3 Nps powder.

AFM technique is used to examine the size, shape, sorption, and structure of nanomaterials as well as their dispersion and aggregation., Fig. 9, 10 and Table 2. showed particle analysis – threshold detection and information with individual results and global statistics of α – Al_2O_3 NPs powder and Fig 11. showed AFM histogram and statistical particle analysis of α – Al_2O_3 NPs powder. length, height and width particle analysis are shown in Fig. 12 and 13. Other particle analysis and topography parameters are shown in Fig 14 – 16 [29- 31].

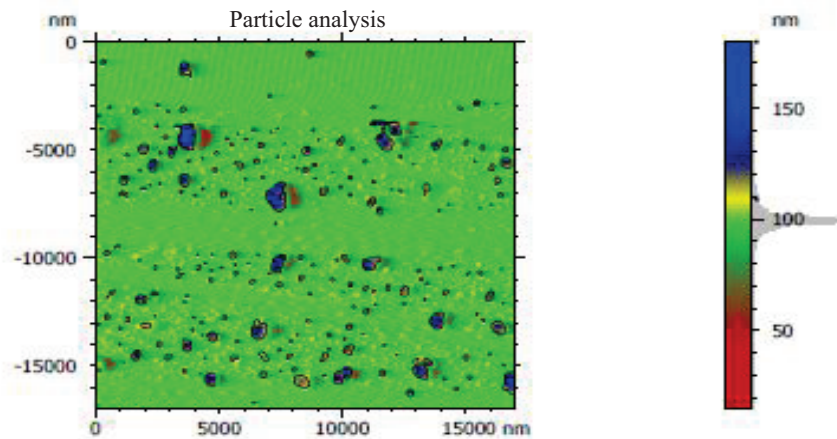


FIGURE 9. AFM particle analysis and threshold detection of α – Al_2O_3 NPs powder.

TABLE 2. AFM information and individual results with global statistics of $\alpha - \text{Al}_2\text{O}_3\text{NPs}$ powder.

Information				
Method	Threshold detection			
Threshold 1	50589	%		
Number of particles	518			
Coverage	4.527	%		
Density	1806152	Particles/mm ²		
Individual results				
Parameters	Projected Area	Projected Area	Mean diameter	Z-maxim
Unit		nm ²	nm	nm
Particle #1	Small	4411	37.79	109.2
Particle #2	Small	4411	37.79	109.3
Particle #3	Small	4411	37.79	109.3
Particle #4	Small	4411	37.79	109.3
Particle #5	Small	4411	37.79	109.3
Particle #6	Small	4411	37.79	109.3
Global statistics				
Mean	*****	25261	97.61	114.7
Min	*****	1240	24.61	109.2
Max	*****	758619	927.7	179.5

MountainsSPIP © Academic 9.2.9994

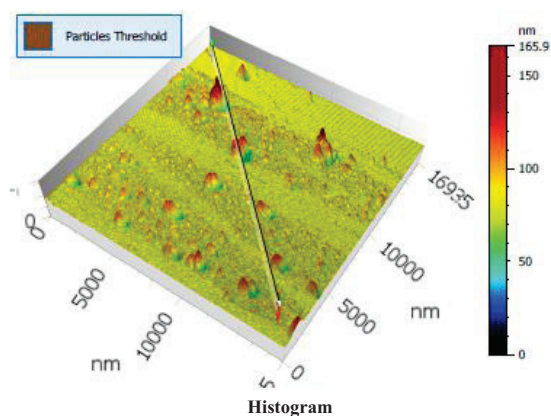


FIGURE 10. AFM image of particle threshold of $\alpha - \text{Al}_2\text{O}_3\text{NPs}$ powder

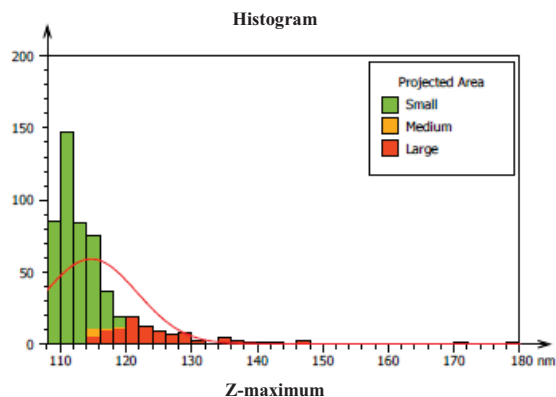


FIGURE 11. AFM histogram and statistical particle analysis of $\alpha - \text{Al}_2\text{O}_3\text{NPs}$ powder.

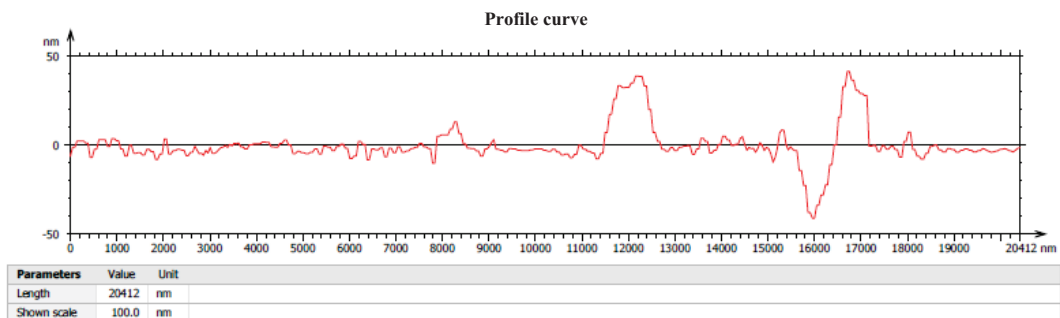


FIGURE 12. AFM curve of particle analysis length of $\alpha - \text{Al}_2\text{O}_3\text{NPs}$ powder.

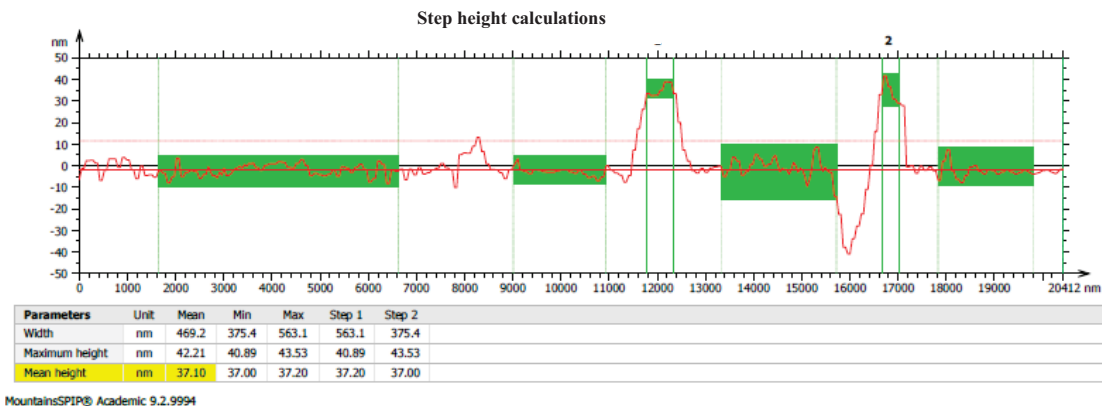


FIGURE 13. AFM height and width calculations parameters of $\alpha - \text{Al}_2\text{O}_3\text{NPs}$ powder.

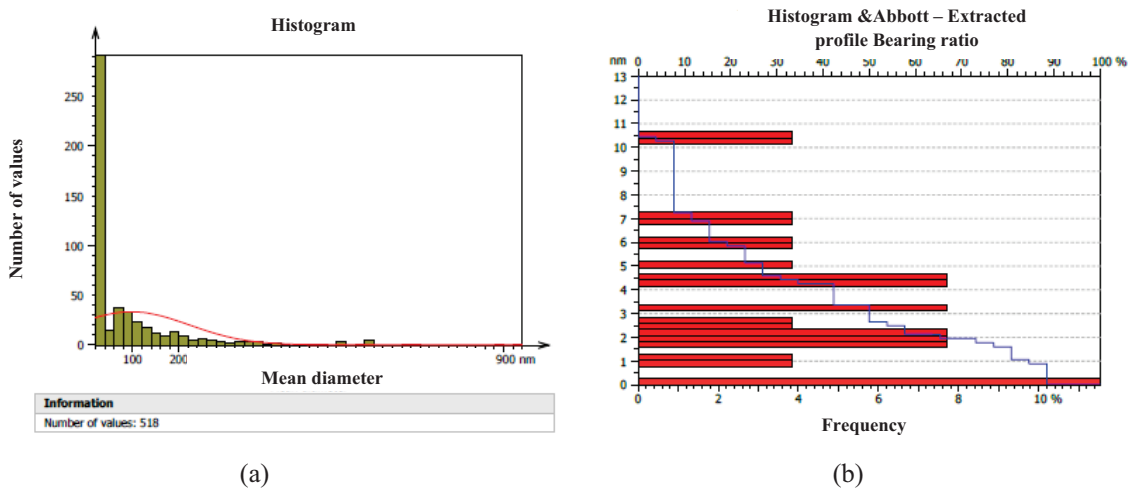
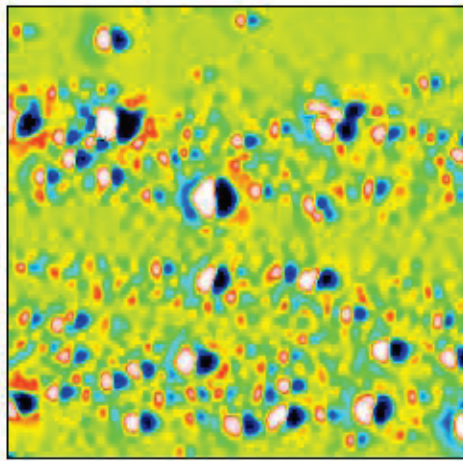
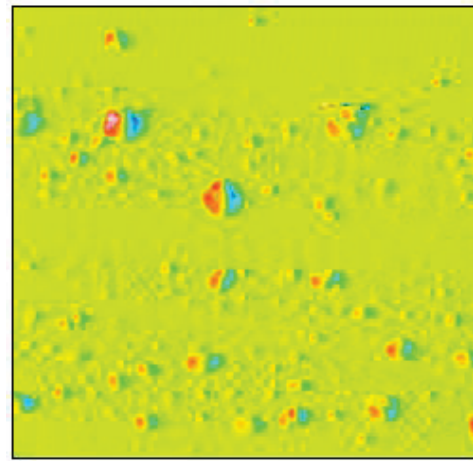


FIGURE 14. AFM a) histogram Number of values against mean diameter, b) abbott curve – extracted profile explain the bearing ratio against frequency of $\alpha - \text{Al}_2\text{O}_3\text{NPs}$ powder.



ISO 25178 – Roughness (S-L)			
F: [Workflow] Form removed (LS poly 3)			
S filter (λ_s): Gaussian, 0.8 μm			
L Filter (λ_c): Gaussian, 0.0025 μm			
Height parameters			
Sq	3.255	nm	Root mean square height
Ssk	0.6125		Skewness
Sku	28.11		Kurtosis
Sp	39.37	nm	Maximum peak height
Sv	31.04	nm	Maximum pit height
Sz	70.42	nm	Maximum height
Sa	1.465	nm	arithmetical mean height
Functional parameters			
Smr	100.0	%	Areal material ratio
Smc	1.792	nm	Inverse areal material ratio
Sdc	3.614	nm	Material ratio higher difference
Hybrid parameters			
Sdq	0.01821		Root mean square gradient
Sdr	0.01654	%	Developed interfacial area ratio

(a)



ISO 25178 – Primary surface			
F: [Workflow] Form removed (LS poly 3)			
F: Leveled (LS), Angle 1.247e10°, 1.023e10°			
S filter (λ_s): None			
Height parameters			
Sq	6.891	nm	Root mean square height
Ssk	0.5325		Skewness
Sku	17.85		Kurtosis
Sp	79.48	nm	Maximum peak height
Sv	84.38	nm	Maximum pit height
Sz	163.9	nm	Maximum height
Sa	3.784	nm	arithmetical mean height
Functional parameters			
Smr	100.0	%	Areal material ratio
Smc	5.467	nm	Inverse areal material ratio
Sdc	10.69	nm	Material ratio higher difference
Hybrid parameters			
Sdq	0.0958		Root mean square gradient
Sdr	0.4498	%	Developed interfacial area ratio

(b)

FIGURE 15. AFM images: [(a) Roughness (S-L), (b) Primary surface] and their topography parameters of α – Al_2O_3 NPs powder.

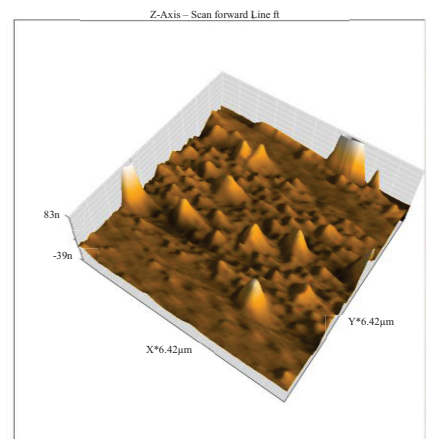
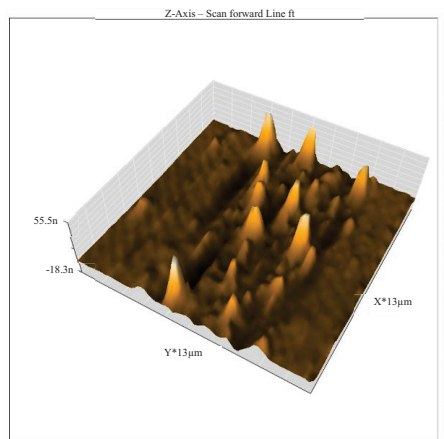


FIGURE 16. 3D surface structure of α – Al_2O_3 NPs powder using AFM.

ANTIBACTERIAL STUDY

Using the approach of agar well diffusion, the antibacterial effectiveness for α - Al_2O_3 Nps was assessed against Escherichia coli, staphylococcus auras, and Candida albicans fungal. The outcomes show that the HCl dilution negative control, and did not exhibit an inhibition zone, indicating that control in its natural state, devoid of nanoparticles, exhibited no antibacterial activity .When the leading of α - Al_2O_3 Nps were (2, 1, 0.5,and 0.25mg/ml), it was found that at all these concentrations , the nanoparticles α - Al_2O_3 caused a growth delay of all bacteria and Candida albicans fungal .Table 3 It showed higher antibacterial activity occurring with a decrease the concentration from (2 to 0.25mg/ml) , while the lower in Candida albicans activity was occurring with a decrease of concentration from (2 to 0.25mg/ml) . [32][33].

TABLE 3. The diameter inhibition zone in (mm) units for sample (A1-A4) α - Al_2O_3 Nps in different concentrations

Sample	A1	A2	A3	A4
Concentrations	2mg/ml	1mg/ml	0.5mg/ml	0.25mg/m
Kind of bacteria	Inhibition area diameter in (mm) for sample (A) α - Al_2O_3 Nps			
<i>E.coli</i>	17mm	19mm	22mm	24mm
<i>S.a</i>	22mm	25mm	27mm	29mm
<i>Ca.bicans</i>	25mm	21mm	20mm	18mm

ADSORPTION STUDY

According to the results of using α - Al_2O_3 Nps as a good removal of various divalent metal ions of (Cobalt, Nickel, and Copper) from a solution of distilled water (See Fig.17).The percentage of the removed ions decreased for α - Al_2O_3 Nps from (93.88 , 85. 67 and 95.90) respectively after (10 min) to (91.25, 84.42 ,and 93.81), indicating the number of active sites available on α - Al_2O_3 Nps. During the first 80 minutes of the adsorption process, the sites on α - Al_2O_3 Nps, the adsorbent gradually became saturated [34][35]. The removal efficiencies of the divalent metal ions of (Cobalt, Nickel, and Copper) were higher as a result of this process, as shown (92.69 % , 84.73%, and 94.97%a) respectively.

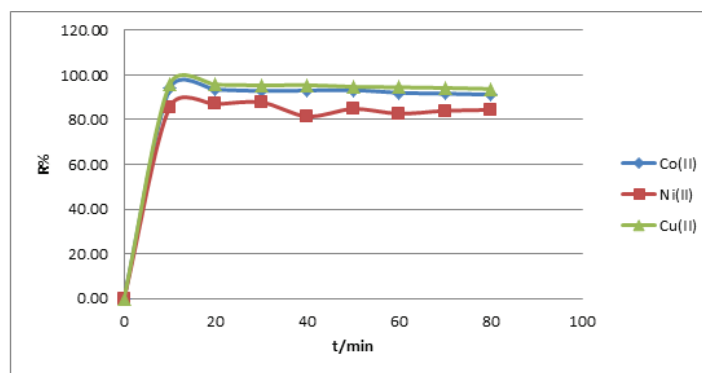


FIGURE 17. Demonstrate the effectiveness of divalent ions of (Ni, Co, and Cu) removal by.

CONCLUSION

α - Al_2O_3 Nps were synthesized by the green method using an aqueous extract of cinnamon. (574 cm^{-1} and 447 cm^{-1}) bands on the Ft-IR spectrum were related to the Al-O bending vibration of the Al-OH groups. the peak at 732 cm^{-1} for octahedral coordinated aluminum's Al-O-Al stretching frequency. The XRD and the morphology study by SEM & TEM showed that the Rhombohedral structure in the sample's crystal structure was consistent with reference patterns in JCPDS files.: 10 – 0173 and 50- 0173. The α - Al_2O_3 Nps morphology had a non-

spherical shape, or a plate-like appearance, and had a uniform size and distribution, with particle size (51.95 – 73.47 nm). AFM showed particle analysis – threshold detection and the topography parameter. The estimates of the optical energy band gap (Eg) were made by U.V–vis spectroscopy which is about $1239.83 / 252 = 4.91$ eV. Al and O were clearly detected by EDX. Alumina was discovered to be chemically pure. α - Al₂O₃Nps antibacterial ability was assessed against (Escherichia coli, staphylococcus aureus and Candida albicans fungal), when the loading of α - Al₂O₃Nps were (2, 1, 0.5, and 0.25 mg/ml), it was found that at all these concentrations, the nanoparticles α - Al₂O₃ caused a growth delay of all bacteria and Candida albicans fungal. The α - Al₂O₃Np has shown excellent adsorbent for Ions Co⁺², Ni⁺² and Cu⁺² so α - Al₂O₃Np absorbs quickly of Co⁺², Ni⁺², and Cu⁺² indicating the presence of active sites and over time, these websites became saturated. So, the creation of simple processes for the synthesis of non-toxic, non-corrosive, eco-friendly nanoparticles using various natural extracts has drawn a lot of attention. The variables that affect the synthesis of nanoparticles and the most appropriate characterization techniques have a significant impact on the quantity and quality of various green nanoparticles. The important and reducing agent in the creation of green nanoparticles and in biological activity and adsorbent is natural extracts.

ACKNOWLEDGMENTS

This work was financially supported by all authors from the University of Baghdad - College of Education of: (pure Science, Ibn – Al – Haitham), Ministry of Education, and Head of Ashur University / Department of: (Medical Laboratory Techniques), Prof. Dr. Falih. H. Musa and also with facilities provided by University of Baghdad, Collage of Education for pure science /Ibn –Al –Haitham, Department of Chemistry.

AUTHOR CONTRIBUTIONS

Waleed. K. Mahdi and Aqeel. O. Flayyih as the corresponding author, worked on the green synthesis of Al₂O₃ nanoparticles. Falih. H. Musa is an idea generator in the formation and application of metal oxide NPs with Waleed. K. Mahdi and Aqeel O. and all authors helped in the synthesis and characterization of nanoparticles. Falih. H. Musa contributed throughout the research and generation of initial reports. All authors have reviewed the manuscript. The authors emphasize the existence of trust, cooperation, and mutual respect during the conduct of research and when working with biological materials, in addition to the available capabilities and applications, as the availability of a cohesive environment is reinforced by ethical considerations, which enabled all parties to participate in all aspects of scientific research.

REFERENCES

1. A. Z. Ziva¹, Y. K. Suryana¹, Y. S. Kurniadianti¹, R. Ragadhita, A. B. D. Nandiyanto, T. Kurniawan, *Mechanical Engineering for Society and Industry*, **1**, 54-77 (2021).
2. A. A. Mohammed, Z. T. Khodair, A. A. Khadom, *Chemical Data Collections* **29**, 100531(2020).
3. W.S.Barakat, O. Elkady, A. Abu-Oqail, H. M. Yehya, A. EL-Nikhaily, *Journal of Petroleum and Mining Engineering* **21**,1-9 (2019).
4. X. Liu, L. Luo, Y. Ding and Y. Xu, *Analyst* **136**, 696-701 (2011).
5. X. Ke, Y. Huang, T. R. Dargaville, Y. Fan, Z. Cui, and H. Zhu, *Separation and Purification Technology* **120**, 239-244 (2013).
6. W. Lin, I. Stayton, Y-W. Huang, X-D. Zhou, and Y. Ma, *Toxicological and Environmental Chemistry* **90**, 983 – 996 (2008).
7. P. A. Prashanth, R. S. Raveendra, R. H. Krishna, S. Ananda, N. P. Bhagya, B. M. Nagabhushana, k. Lingaraju, and H. R. Naika, *Journal of Asian Ceramic Societies* **3**, 345 – 351 (2015).
8. Y. Hakuta, N. Nagai, Y-H. Suzuki, T. Kodaira, K. K. Bando¹, H. Takashima, and F. Mizukami " Preparation of α -alumina nanoparticles with various shapes via hydrothermal phase transformation under supercritical water conditions " Conference. Series: Materials Science and Engineering (Published by IOP Publishing, 2013), pp. 1-4.
9. S. A. Al-Mamun, R. Nakajimab, and T. Ishigak, *Journal of Colloid and Interface Science*. **392**, 177- 182 (2013).
10. H. Gao, Z. Li, and P. Zhao, *Modern Physics Letters B*, **32**,1850109 (2018).
11. A. Rajaeiyan, and M. Bagheri-Mohagheghi, *Advances in Materials Science and Engineering* **2013**, 1-9 (2013).
12. S. Ghotekar, Nano chemistry Research, Review Paper **4**, 163 - 169 (2019).

13. S. Ravichandran, R. D. Durai, P. D. Krishnan, P. Rameshkumar, T. Thomas, S. N. Narayanan, B. Hosnedlova, B. Havelkova, M. Jakubek, M. Beklova, R. Kizek, and V. H. B. Narayanan "preparation of Aluminum oxide nanoparticles using green synthesis ", conference proceeding (published by nanocon, 2021), pp. 337- 343.
14. R. Ismail, S. Zaidan, and R. M. Kadhim, *Applied Nanoscience* **46**, 477 – 487, (2017).
15. V. M. Narayanan, and S. G. Rakesh, " Synthesis of colloidal alumina nanoparticles using green method "IOP Conference. Series: Materials Science and Engineering (Published by IOP Publishing, 2018), pp. 1-9.
16. D. Manyasree, P. Kiranmayi, and Ravikumar, R. V. S. S. N. b, *International Journal of Pharmacy and Pharmaceutical Sciences*, **10**, 32-35 (2018).
17. S. Pakrashi, S. Dalai, D. Sabat, S. Singh, N. Chandrasekaran, and A. Mukherjee, *Chemical Research in Toxicology* **24**, 1899-1904 (2011).
18. P. Nagarajan, V. Subramaniyan, V. Elavarasan, N. Mohandoss, P. Subramaniyan, and S. Vijayakumar, *Sustainability* **15**, 1-9(2023).
19. S. Narayanan, N. Baskar, V. H. BN, R. Sankaran and R. Devi D, *Scientific Reports* **9**, 17803 (2019).
20. A. I. Y. Tok, F. Y. C. Boey, and X. L. Zhao, *Journal of Materials Processing Technology* **178**, 270 – 273 (2006).
21. A. Boumaza, A. Djelloul, and F. Guerrab, *Powder Technology*, **201**, 177- 180 (2010).
22. C. Ma, Y. Chang, W. Ye, W. Shang, and C. Wang, *Journal of Colloid and Interface Science*. **317**, 148–154 (2008).
23. J. Roy, N. Bandyopadhyay, S. Das, and S. Maitra, *Iranian Journal of Chemistry* **30**, 65– 71 (2011).
24. A. F. Alamouti, M. Nadafan, Z. Zehghani, A. Vejdani- Noghreiyani, and M. H. Majlesara, *Journal of Asian Ceramic Societies*. **9**, 1-8 (2021) .
25. A. N. Saud, H. Sh. Majdi, S. N. Saud, *Cerâmica*. **65**, 236-239 (2019).
26. N. Varghese, M. Hariharan, A. B. Cherian, P. V. Sreenivasan, J. Paul, and A. Antony, PVA-Assisted synthesis and characterization of nano α -alumina, *International Journal of Scientific and Research* **4**, 1-4 (2014).
27. T. Sabah, K. H. Jawad, and N. Al-attar, *Research Journal of Pharmacy and Technology* **16**, 1267-1273 (2023).
28. K. Djebaili, Z. Mekhalif, A. Boumaza, and A. Djelloul, *Journal of spectroscopy* **2015**, 1-16 (2015).
29. M. Cascione, V. De Matteis, V. F. Persano, and S. Leporatti, *materials* **15**, 1-12 (2022) .
30. D. Hill, A. R. Barron, and S. Alexander, *Journal of colloid and interface science* **567**, 45- 53 (2020).
31. M. Ranjbar, G. D. Noudeh, M-A. Hashemipour, I, and Nanomedicine, and Biotechnology **47**, 201 – 209 (2019).
32. A. S. Jawad, Q. N. Thewaini, and S. Al-Musawi, *Journal of Applied Sciences and Nanotechnology* **1**, 42- 50 (2021).
33. A. O. Flayyih , W . K. Mahdi, Y. I.M. Abu zaid, and F. H. Musa, *Chemical Methodologies* **6**, 620 - 628 (2022).
34. C. Prochaska, and G. Gallios, *Processses* **9**, 1-23(2021).
35. Z. Bonyadi , Z Fouladi , A . Robotjaz, and M. Z. Anbarani, *Applied Water Science* **52** ,1- 11 (2023) .